

Depth-Weighted Detection of Behaviours of Risk in People with Dementia using Cameras

Pratik K. Mishra, Irene Ballester, Andrea Iaboni, Bing Ye, Kristine Newman, Alex Mihailidis, and Shehroz S. Khan

Abstract—The behavioural and psychological symptoms of dementia, such as agitation and aggression, present a significant health and safety risk in residential care settings. Many care facilities have video cameras in place for digital monitoring of public spaces, which can be leveraged to develop an automated behaviours of risk detection system that can alert the staff to enable timely intervention and prevent the situation from escalating. However, one of the challenges in our previous study was the presence of false alarms due to obstruction of view by activities happening close to the camera. To address this issue, we proposed a novel depth-weighted loss function to train a customized convolutional autoencoder to enforce equivalent importance to the events happening both near and far from the cameras; thus, helping to reduce false alarms and making the method more suitable for real-world deployment. The proposed method was trained using data from nine participants with dementia across three cameras situated in a specialized dementia unit and achieved an area under the curve of receiver operating characteristic of 0.852, 0.81 and 0.768 for the three cameras. Ablation analysis was conducted for the individual components of the proposed method and the performance of the proposed method was investigated for participant-specific and sex-specific behaviours of risk detection. The proposed method performed reasonably well in detecting behaviours of risk in people with dementia motivating further research toward the development of a behaviours of risk detection system suitable for deployment in video surveillance systems in care facilities.

Index Terms—Dementia, Behaviours of risk, Agitation,

This paragraph of the first footnote will contain the date on which you submitted your paper for review. This work was supported by AGE-WELL NCE Inc, Alzheimer's Association, Natural Sciences and Engineering Research Council, UAE Strategic Research Grant, Walter and Maria Schroeder Institute for Brain Innovation and Recovery and the European Union's Horizon 2020 research and innovation programme under MSCA grant agreement number 861091 for the visuAAL project.

Pratik K. Mishra, Alex Mihailidis and Shehroz S. Khan are with KITE, Toronto Rehabilitation Institute, Toronto, ON, Canada, and Institute of Biomedical Engineering, University of Toronto, Toronto, ON, Canada (e-mail: pratik.mishra@mail.utoronto.ca; alex.mihailidis@utoronto.ca; shehroz.khan@uhn.ca).

Irene Ballester is with Computer Vision Lab, TU Wien, 1040 Vienna, Austria (e-mail: irene.ballester@tuwien.ac.at)

Andrea Iaboni is with KITE, Toronto Rehabilitation Institute, Toronto, ON, Canada, and Department of Psychiatry, Temerty Faculty of Medicine, University of Toronto, Toronto, ON, Canada. (e-mail: andrea.iaboni@uhn.ca)

Bing Ye is with KITE, Toronto Rehabilitation Institute, Toronto, ON, Canada. (e-mail: bing.ye@utoronto.ca)

Kristine Newman is with Daphne Cockwell School of Nursing, Toronto Metropolitan University, Toronto, ON, Canada. (e-mail: kristine.newman@torontomu.ca)

Video, Autoencoder, Anomaly Detection, Deep Learning.

I. INTRODUCTION

People living with dementia (PwD) can develop behavioural and psychological symptoms putting themselves and the people around them at risk. These behaviours of risk include pacing, pushing, hitting, kicking, intentional falling, and other behaviours that are self-harming, or harmful to others [1]. Long term care (LTC) homes often suffer from understaffing [2] making it challenging for the staff to continuously oversee the safety of the residents. Video cameras are an unobtrusive and inexpensive alternative for monitoring behaviour as they are already used by many LTC homes for security purposes, saving the time and expense of additional infrastructure installation. Video cameras are rich in vital spatio-temporal information, which can be leveraged using deep learning approaches to design automated behaviours of risk detection systems that can be used to alert the staff in real-time and enable timely and appropriate interventions. This has important implications for safety and for helping to better understand the nature and triggers of the behaviours.

Behaviours of risk detection is a challenging problem due to their diversity and rare occurrence, making supervised classification approaches inappropriate. An anomaly detection approach is more plausible, where a method can be trained to learn the normal behaviour characteristics and identify high variation cases as anomalies during testing [3]. In our previous work [4], a spatio-temporal autoencoder was used to detect behaviours of risk as anomalies in a single dementia participant and a single camera. However, there were significant issues with false positives (or false alarms), that could cause usability issues. In general, video anomaly detection (VAD) autoencoder approaches can become sensitive to the background, leading to high reconstruction errors when a major part of the background is blocked [5]. The objects or people closer to the camera cover a larger portion of the background than those further away, leading to significantly higher reconstruction errors and causing increased false positives. To tackle this problem, we propose a novel loss function where the depth of the pixels is used as weight to diminish the overshadowing effect caused by the larger area of the people/objects close to camera. The aim is to reduce false positives by enforcing equivalent importance in analyzing the events happening in the unit irrespective of the distance to camera. Further, in the absence of anomalies

in the training set, we propose to utilize unusual activities that are not behaviours of risk, such as large objects or crowded scenes as proxy outliers to determine a threshold for detecting behaviours of risk. The performance for detecting behaviours of risk can vary across individuals depending upon the type of behaviours of risk, number of episodes recorded and demographic variables such as sex. To address this variability, we also conduct participant-specific and sex-specific analyses of the effectiveness of detecting behaviours of risk by the proposed method. The main contributions of this work are:

- 1) We propose a novel depth-weighted loss function, where pixel depth is used to enforce equivalent importance to both near and far events and reduce the false positives.
- 2) We use the outlier activities in the training data to determine a threshold. We expand our analysis to nine participants with dementia and three different cameras.
- 3) We conduct an ablation analysis to investigate the effectiveness of individual components of the proposed method in detecting behaviours of risk in PwD.
- 4) We perform experiments to analyze the performance of the proposed method for participant-specific and sex-specific behaviours of risk detection in PwD.

II. RELATED WORK

In this section, we present the existing work for detecting behaviours of risk in PwD using videos and handling false positives in VAD scenarios.

Behaviours of Risk Detection: The current approaches for detecting behaviours of risk in PwD use different types of modalities, including wearable devices [6], computer vision [4], [7], radio waves [8] and multimodal / ambient sensing [9]. As this work uses videos, further review only discusses the studies that either use videos alone or in combination with other sensors. Qiu et al. [9] proposed a multimodal information fusion model using various sensors, including pressure sensors, ultrasound sensors, infrared sensors, video cameras, and acoustic sensors. A layered classification architecture, consisting of a hierarchical hidden Markov model and a support vector machine, was employed. However, their results were based on mock-up data generated through simulation. Chikhaoui et al. [10] developed an ensemble learning classifier to detect agitation using data from a Kinect camera and an accelerometer. Ten participants were instructed to perform six different agitated and aggressive behaviours. However, the study did not specify whether the participants were healthy volunteers or PwD. Fook et al. [7] introduced a method employing a multi-layer architecture of a probabilistic classifier based on hidden markov model and a support vector machine classifier. However, the video data involved a person in bed, and it was unclear whether the participants were healthy individuals or PwD. For all the above studies, it appears that these systems were conceptual and were never tested with real patients, so their performance is unknown in a real-world setting. Acknowledging the importance of employing real-world data, in our previous work, we proposed an unsupervised convolutional autoencoder to detect agitation in PwD using videos collected from a specialized dementia unit from a single

participant and a single camera [11]. In our later work [4] with the same limited dataset, we presented privacy-protecting VAD approaches to detect behaviours of risk in PwD using body pose information for the participants or semantic segmentation masks.

Reducing False Positives: A VAD method can land into usability issues in the presence of increased false positives. Therefore, it is important to assess the rate of false positives (or false alarms) in these applications. We briefly review existing methods that handle false positives for VAD scenarios. Doshi and Yilmaz [12] proposed an online VAD method and a procedure for selecting an operating threshold that satisfied a desired false alarm rate. The framework was composed of deep learning-based feature extraction from video frames and a statistical sequential anomaly detection algorithm. Zhou et al. [13] proposed an anomaly trajectory detection framework for online traffic incident alerts on freeways. It used an adversarial loss to enable the autoencoder to learn a better normal trajectory pattern that is beneficial for reducing false alerts, while an abnormal trajectory discriminator was established and trained to detect small mean shifts and filter out instantaneous false alerts. Mozaffari et al. [14] proposed an online and multivariate anomaly detection method that was suitable for the timely and accurate detection of anomalies. They analyzed an asymptotic false alarm rate and provided a procedure for selecting a threshold to satisfy a desired false alarm rate. Singh et al. [15] aimed to address the challenge of a high false alarm rate resulting from the trade-off between learning to reconstruct and distinguish anomalies. They proposed a constrained generative adversarial network where white gaussian noise was added to the input to boost the robustness of the model.

The existing methods tried to reduce false positives by leveraging algorithmic designs or choosing the threshold depending on a desired false positive rate. However, as described in Section I, the obstruction caused depending on the distance of objects/people from the camera can be a determinant factor in the increased false positives in VAD tasks. Hence, we utilize the depth of pixels to handle this issue and enforce equivalent importance to events happening far and close to the camera, thus reducing the false positives.

III. METHODS

A. Data Collection

The video data used in this work was collected as part of a larger multimodal sensor study [6] at the Specialized Dementia Unit (SDU) at Toronto Rehabilitation Institute, University Health Network (UHN), Toronto, Canada, between November 2017 and October 2019. The participants were admitted to the SDU from long-term care homes for the evaluation and management of behavioural and psychological symptoms in advanced dementia. Inclusion criteria encompassed individuals aged over 55 years, diagnosed with dementia and with a history of agitation or aggressive behaviours. The participants who expressed dissent toward wearing the sensor device were excluded from the study. Data collection ceased under either of the following circumstances: absence of documented agitation for one week, repeated removal of the wristband, sickness,

death or discharge from the unit, or upon completion of two months of data collection. The data collection was approved by the research ethics board (UHN REB#14-8483). Informed consent was obtained from substitute decision-makers for all participants. The staff also provided written consent for video recording within the unit. Additionally, all staff and decision-makers of participants shown in the images in the paper have granted written consent for the publication of their images.

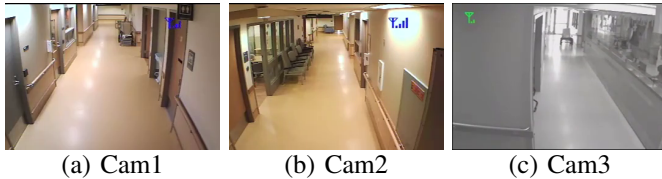


Fig. 1: Different camera views.

TABLE I: Participants’ demographic information.

Attribute	Value
Number of Participants	9
Median age of participants (years)	82
Mean age of participants (years)	81.22
Standard deviation of the age of participants (years)	8.12
Range of age of participants (years)	66–93
Gender	Males (3) Females (6)

B. Selected Dataset

For this study, we selected a subset from the larger video dataset comprising the top three cameras (see Fig. 1) based on the maximum documented behaviours of risk events. Table I presents the demographic information of the participants. The selected video data captured the behaviours of risk events for nine dementia participants with an age range of 66–93 years and a mean age of 81.22 ± 8.12 years. There were three male and six female participants.

C. Data Annotation

Two research assistants independently reviewed the selected videos 30 minutes before and after the documented behaviours of risk events and annotated all the events corresponding to motor or physical agitation. Due to the lack of audio during data collection, it was not possible to annotate verbal aggression. Anvil [16] tool was used for the annotation of camera videos. Both the research assistants annotated the videos separately for the presence of behaviours of risk events and other activities, namely, the presence of unusual activities, crowded scenes and large objects. The two research assistants individually annotated 305 and 383 behaviours of risk events across three cameras and nine participants. For the final labelling, an event was labelled as behaviour of risk if either of the research assistants annotated it as a behaviour of risk. For cases where both the assistants annotated an event as behaviour of risk but disagreed in the start/end times of the annotation, the duration with common agreement was labelled as a behaviour of risk. An inter-rater agreement analysis was

TABLE II: Size of training and test sets (in minutes).

	Cam1	Cam2	Cam3
Train set	1225.25	1242.33	1205.66
Test set	209.16	291.92	96
Normal behaviour (Test set)	194.08	270.5	89.83
Behaviours of risk (Test set)	15.08	21.42	6.17

performed, where Cohen’s kappa [17], Krippendorff alpha [18] and percentage agreement metrics were calculated over the annotations of both research assistants. This was done to measure the agreeability of the two annotations over the categorization of the events into normal and behaviours of risk events. The Cohen’s kappa, Krippendorff alpha and percentage agreement were determined as 0.48, 0.48 and 0.99, respectively. The value of Cohen’s kappa and Krippendorff alpha can range from -1 to 1 , where 1 and -1 represent a perfect agreement and disagreement, and 0 represents the amount of agreement expected from random chance. A score between 0.41 to 0.60 for Cohen’s kappa is considered as moderate [17].

D. Data Preprocessing

The frames were sampled from the videos at 15 frames per second, converted to grayscale, normalized to range $[0, 1]$ (pixel values divided by 255) and resized to 64×64 resolution – this was done to minimize the computational expenses associated with trainable parameters. The frames were then stacked separately to form non-overlapping 5-second windows (75 frames per window) (based on previous work [11]). The labels for behaviours of risk were refined in accordance with the 5-second windows. Training and test sets were generated individually for the three cameras. The training sets were composed of normal behaviours from daily activities only. The test sets were composed of both normal and behaviours of risk events. The training set size was fixed around an average of 1224.41 minutes across three cameras. The test set consists of a combination of behaviours of risk events from nine participants across three cameras along with normal behaviours. In the test sets, the available duration of annotated behaviours of risk events was limited. Hence, the duration of normal behaviour in test sets was chosen to keep a similar imbalance ratio (as in previous work [4]), which is approximately 7% for behaviours of risk events. Table II shows the size of training and test sets for each of the three cameras. The number of 5-second windows and types of behaviours of risk across participants and cameras in the test set are presented in Table III.

E. Behaviours of Risk Detection

Spatio-temporal convolutional autoencoders (3DCAE) learn to reconstruct the input videos by minimizing the reconstruction error during training. The intuition is that 3DCAE is trained to reconstruct only normal instances. During testing, normal instances will have a lower reconstruction error, while instances with high reconstruction error are treated as anomalies (behaviours of risk in our case). Previously, a customized 3DCAE was used to detect behaviours of risk from data from one participant and a single camera [4], [11].

TABLE III: Number of 5-second windows and types of behaviours of risk across participants and cameras in test set.

Participant#	Sex	Cam1	Cam2	Cam3	Type of behaviour of risk
Participant1	F	17	25	12	Hitting, Pushing, Falling, Kicking, Grabbing, Throwing, Other
Participant2	F	3	3	1	Pushing, Other
Participant3	M	15	26	15	Hitting, Pushing, Kicking, Grabbing, Other
Participant4	F	121	199	44	Hitting, Pushing, Kicking, Grabbing, Throwing, Other
Participant5	F	0	0	1	Hitting, Pushing, Kicking, Other
Participant6	M	17	0	1	Hitting, Pushing, Kicking, Grabbing, Other
Participant7	F	8	0	0	Pushing, Grabbing, Other
Participant8	F	0	3	0	Pushing, Other
Participant9	M	0	1	0	Hitting, Grabbing, Other

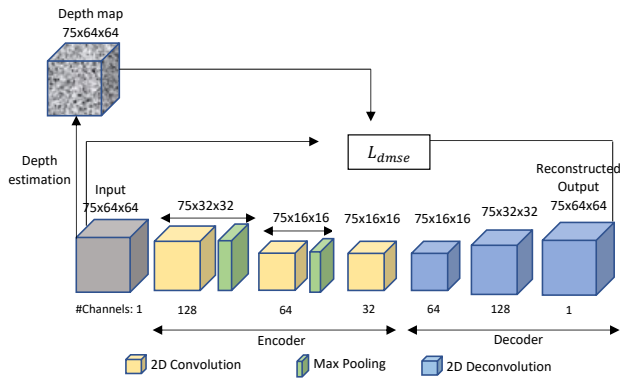


Fig. 2: depCAE architecture to detect behaviours of risk.

However, previous approaches showed high false positives due to obstruction caused by activities such as crowded scenes, large objects, or other events happening near the camera due to reasons described in Section I. Such instances are extremely common in normal day-to-day activities happening in care units. As such, there was a need to handle this issue to make the method suitable for real-world deployment. Hence in this work, we propose a novel depth-weighted loss function to train a convolutional autoencoder, depCAE, where the depth of the pixels is used as a weight factor to enforce equivalent importance to both behaviours of risk and non-behaviours of risk events happening far and near the camera. It is hypothesized that the weighted-depth loss function will lead to a reduction in false positives in this problem. We also propose a new method to determine the threshold for detecting behaviours of risk as anomalies using the abnormal non-behaviours of risk activities in the training set as outliers.

The depCAE followed an encoder-decoder architecture, where the encoder consisted of 2D convolution and max-pooling layers, with a kernel size of $(1 \times 3 \times 3)$, stride $(1 \times 1 \times 1)$ and padding $(0 \times 1 \times 1)$, followed by batch normalization and ReLU operations. The decoder used 2D deconvolution layers (2D transposed convolution operation) with a kernel size of $(1 \times 3 \times 3)$, strides $(1 \times 1 \times 1)$, $(1 \times 2 \times 2)$, $(1 \times 2 \times 2)$ and paddings $(0 \times 1 \times 1)$, $(0 \times 1 \times 1)$, $(0 \times 1 \times 1)$ for first, second, and third 2D deconvolution layers, respectively. The overall architecture of the depCAE is presented in Fig. 2.

Depth-weighted Anomaly Score: Existing CAE meth-

ods [4] employ reconstruction error to detect anomalous frames. This strategy inherently favours anomalies closer to the camera, as they occupy more pixels in the image plane. This bias poses a challenge, especially in scenes with highly varying distances from the camera, such as corridors (see Fig. 1). As a result, anomalies at different distances receive unequal anomaly scores, with those closer to the camera being unfairly favoured. To address this problem, we propose a loss function where depth per pixel is used as weight during the calculation of reconstruction error to enforce equivalent importance to both near and far pixels.

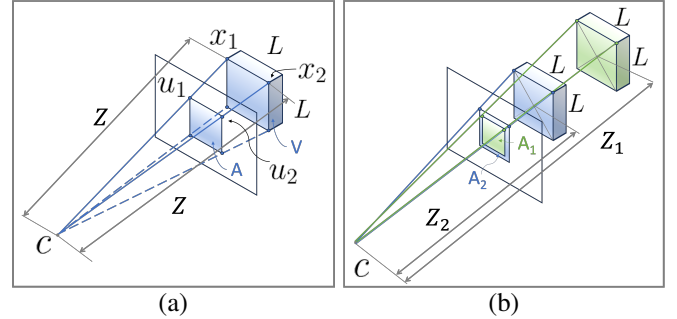


Fig. 3: (a) Illustration of the geometric relationship between volume and area of the projected square into the image plane. (b) Derivation of the relationship between projected areas at different distances from the camera.

To understand the translation of an anomaly in 3D space, we describe the relationship between the area A depicting the anomaly in the image and its 3D volume. For simplicity, consider this volume as a square prism with dimensions equal to L (see Fig. 3 (a)). Consider now two of the vertex of the square prism represented by two 3D points $x_1 = (X_1, Y_1, Z_1)$ and $x_2 = (X_2, Y_2, Z_2)$ in the 3D space and their 2D projections $u_1 = (U_1, V_1)$ and $u_2 = (U_2, V_2)$. The projection of a 3D point onto a 2D image plane is expressed by the image coordinates (U, V) , related to the 3D world coordinates (X, Y, Z) through the pinhole camera model equations:

$$U = \frac{fX}{Z}, \quad V = \frac{fY}{Z} \quad (1)$$

where f is the focal length and Z is the distance from the 3D point to the camera position. Assuming the difference in depth Z between these points is negligible ($Z \approx Z_1 \approx Z_2$), the projections on the image plane according to equation (1) are:

$$U_1 = \frac{fX_1}{Z}, \quad U_2 = \frac{fX_2}{Z} \quad (2)$$

Given that the distance between the points in the 3D space along the X-axis is $L = |X_2 - X_1|$, the area A of the square in the 2D plane containing the anomaly is:

$$A = (U_2 - U_1)^2 = \left(\frac{f}{Z}\right)^2 (X_2 - X_1)^2 = \left(\frac{fL}{Z}\right)^2 \quad (3)$$

To analyze the sensitivity of the anomaly score (AS) on the distance from the camera and therefore, on the area in the

image plane, we can express the anomaly score $(AS)^A$ of an area A as:

$$(AS)^A = \overline{(AS)^{\text{pixel}}} \cdot A \quad (4)$$

where $\overline{(AS)^{\text{pixel}}}$ represents the average anomaly score per pixel, a constant value that depends solely on the anomaly itself, irrespective of its position in 3D space or its projection onto the image plane.

Consider the same anomaly event, i.e., same value of $\overline{(AS)^{\text{pixel}}}$, at different distances Z_1 and Z_2 from the camera. As illustrated in Fig. 3 (b), this results in different area values A_1 and A_2 in the image plane, with $A_1 < A_2$ if $Z_1 > Z_2$. Since both anomalies have the same value of $\overline{(AS)^{\text{pixel}}}$, according to equation (4), the difference in area will result in a different anomaly score. To ensure depth invariance, we need the anomaly to have the same score AS_{inv} regardless of its distance from the camera. This is achieved by introducing a factor K :

$$AS_{inv} = K_1 \cdot (AS)^{A_1} = K_2 \cdot (AS)^{A_2} \quad (5)$$

Combining the equations (3), (4) and (5), and since $\overline{(AS)^{\text{pixel}}}$ is a constant, we can express AS_{inv} as:

$$AS_{inv} = K_1 (fL)^2 \frac{1}{Z_1^2} = K_2 (fL)^2 \frac{1}{Z_2^2} \quad (6)$$

Therefore, given the constant value of $(fL)^2$, to achieve depth invariance, the factors K_1 and K_2 must satisfy the following conditions:

$$K_1 = Z_1^2, \quad K_2 = Z_2^2 \quad (7)$$

Based on this, we propose the following novel loss function where depth per pixel is used as weight during the calculation of reconstruction error as a depth-weighted mean squared error to enable depCAE to enforce equivalent importance to both near and far pixels.

$$L_{dmse} = \frac{1}{N_e} \sum_{l=1}^W \sum_{i=1}^S \sum_{j=1}^S Z_{l,i,j} (I_{l,i,j} - O_{l,i,j})^2 \quad (8)$$

where, I is the input pixel, O is the reconstructed pixel, Z is the pixel depth, S is the spatial size, W represents the number of frames in a window and is termed as the window size and N_e is the total number of pixels in a window. In the depCAE method, $W = 75$ and $N_e = 75 \times 64 \times 64 = 307200$. Empirically, we found that using a weight Z in equation (8) gave better performance than the weight Z^2 . The weighted-depth loss function helped the method to treat both the near and far behaviours of risk events with similar importance, which in turn helped to reduce false positives. The depth map was estimated using the work by Ranftl *et al.* [19]. During testing, the depth-weighted mean squared error was used as anomaly score for detecting behaviours of risk.

Threshold Determination: In an anomaly detection approach, it can be challenging to determine an operating threshold due to the absence of anomalous samples in the training set. As discussed in Section III-C, the data was annotated

for other unusual activities, such as large objects, crowded scenes and other infrequent activities in the training set. Due to the unusual nature of these annotated activities relative to the activities of daily living in a dementia unit, we propose to treat these activities as proxy outliers to create a proxy validation set to determine the threshold. Following a similar approach as Khan *et al.* [20], we chose the training reconstruction error with maximum F1-score on proxy validation set as the operating threshold.

Performance Evaluation: The primary metric employed for evaluating the performance of methods was the area under the curve of receiver operating characteristic (AUROC), supplemented by F1-score. Additional metrics are also reported, including true positive rate (TPR), true negative rate (TNR), false positive rate (FPR), false negative rate (FNR), $g\text{mean}(\sqrt{TPR * TNR})$, Matthew's Correlation Coefficient (MCC), precision, recall, specificity, and balanced accuracy [21]. Transformers and variational autoencoders have performed well in the existing literature for the task of VAD [22], [23]. Hence, in addition to the baseline 3DCAE method [4], the performance of the depCAE for detecting behaviours of risk in PwD as anomalies was compared with two additional existing methods, namely a self-supervised masked convolutional transformer [22] block-based autoencoder 3DCAE.SSMCTB and a variational autoencoder VAE [24]. The 3DCAE.SSMCTB method used a self-supervised masked convolutional transformer block [22] embedded after the encoder layer and its output was passed as input to the decoder. The transformer block [22] was structured as a convolutional layer with dilated masked kernels, followed by a transformer module that performed channel attention. A self-supervised loss function was used with the block to minimize the reconstruction error between the masked input and the predicted output. VAE [24] learned to generate two vectors that represent the parameters (mean and variance) of a distribution from which the latent vector was sampled instead of learning how to generate a latent vector that the decoder function can reproduce. For fairness during comparison, the encoder and decoder architecture of 3DCAE, 3DCAE.SSMCTB and VAE was kept the same as depCAE and they used interquartile range (IQR) generated proxy-validation set [20] for threshold calculation.

IV. RESULTS AND DISCUSSION

In this section, we present the results to gauge the effectiveness of depCAE in detecting behaviours of risk in PwD and compare its performance with existing methods 3DCAE, 3DCAE.SSMCTB and VAE. We further conducted an ablation analysis of different components of the depCAE method and performed participant and sex-specific analysis of depCAE performance.

Performance Comparison: Table IV shows the performance of depCAE compared to other methods for the detection of behaviours of risk in PwD across three cameras. The best values for the primary performance metrics AUROC and F1-score are marked in bold. The cases where depCAE gave lower FPR as compared to baseline 3DCAE method are marked in

TABLE IV: Performance of different methods for behaviours of risk detection in PwD on three different cameras.

Metric	Cam1				Cam2				Cam3			
	3DCAE	3DCAE-SSMCTB	VAE	depCAE	3DCAE	3DCAE-SSMCTB	VAE	depCAE	3DCAE	3DCAE-SSMCTB	VAE	depCAE
TPR	0.945	0.950	0.641	0.939	0.949	0.728	0.502	0.844	0.919	0.649	0.230	0.730
TNR	0.628	0.581	0.713	0.684	0.611	0.668	0.812	0.686	0.530	0.645	0.903	0.714
FPR	0.372	0.419	0.287	0.316	0.389	0.332	0.188	0.314	0.470	0.355	0.097	0.286
FNR	0.055	0.050	0.359	0.061	0.051	0.272	0.498	0.156	0.081	0.351	0.770	0.270
Gmean	0.770	0.743	0.676	0.801	0.761	0.697	0.638	0.761	0.698	0.647	0.455	0.722
MCC	0.301	0.276	0.198	0.335	0.295	0.215	0.200	0.290	0.220	0.149	0.105	0.235
Precision	0.165	0.150	0.148	0.187	0.162	0.148	0.174	0.176	0.118	0.111	0.139	0.149
Recall	0.945	0.950	0.641	0.939	0.949	0.728	0.502	0.844	0.919	0.649	0.230	0.730
Specificity	0.628	0.581	0.713	0.684	0.611	0.668	0.812	0.686	0.530	0.645	0.903	0.714
Balanced Accuracy	0.786	0.765	0.677	0.811	0.780	0.698	0.657	0.765	0.724	0.647	0.566	0.722
F1-score	0.281	0.259	0.240	0.313	0.276	0.246	0.259	0.291	0.210	0.190	0.173	0.248
AUROC	0.844	0.779	0.754	0.852	0.810	0.766	0.790	0.810	0.765	0.739	0.709	0.768

TABLE V: Ablation analysis of proposed components across three different cameras.

Metric	Cam1			Cam2			Cam3		
	depWgtOnly	anntThrOnly	depCAE	depWgtOnly	anntThrOnly	depCAE	depWgtOnly	anntThrOnly	depCAE
Gmean	0.760	0.805	0.801	0.743	0.791	0.761	0.624	0.647	0.722
MCC	0.294	0.344	0.335	0.269	0.325	0.290	0.167	0.172	0.235
Precision	0.158	0.202	0.187	0.158	0.188	0.176	0.098	0.135	0.149
Recall	0.967	0.895	0.939	0.879	0.907	0.844	0.905	0.554	0.730
specificity	0.598	0.725	0.684	0.628	0.690	0.686	0.430	0.756	0.714
Balanced Accuracy	0.782	0.81	0.811	0.754	0.798	0.765	0.668	0.655	0.722
F1-score	0.271	0.32	0.313	0.267	0.311	0.291	0.177	0.217	0.248
AUROC	0.851	0.842	0.852	0.802	0.81	0.81	0.765	0.768	0.768

gray cells. Our depCAE method achieved the best AUROC and F1-score for all three cameras in comparison to other methods. The depCAE method achieved an AUROC and F1-score of 0.852 and 0.313 for Cam1, 0.81 and 0.291 for Cam2, and 0.768 and 0.248 for Cam3. Further, our depCAE method gave lower FPR as compared to 3DCAE and 3DCAE.SSMCTB methods for all three cameras. This shows that the proposed idea of using pixel depth as weight in the loss function is indeed effective in reducing false positives. The depCAE method performed better for Cam1 and Cam2 in comparison to Cam3, which can be attributed to the major portion of Cam3 view being occluded by the wall. This made it difficult to gauge the behaviours of risk events clearly in Cam3.

Ablation Analysis: We investigated the relative effectiveness of the two components of the proposed method, namely, depth-weighted loss function and threshold determination using annotated outliers, in detecting behaviours of risk in PwD. Table V presents the results for ablation analysis over three cameras, where depWgtOnly refers to the setting of depCAE trained using depth-weighted loss function while using IQR outliers [20] for threshold calculation, and anntThrOnly refers to the setting of using mean squared error loss function while using annotated outliers for threshold calculation. The best AUROC and F1 scores are marked in bold. For Cam1, anntThrOnly performed better than depWgtOnly in terms of F1-score, while depWgtOnly performed better in terms of AUROC. Overall, depCAE benefited from combined performance of depWgtOnly and anntThrOnly giving an AUROC of 0.852. For Cam2, anntThrOnly performed similar to depCAE in terms of AUROC, while the performance of depCAE degraded in comparison to anntThrOnly in terms of F1-score. For Cam3, depCAE benefited from the combined functionality of depWgtOnly and anntThrOnly, outperforming both of them in

terms of F1-score and AUROC. Overall, it can be observed that both depWgtOnly and anntThrOnly are vital components of depCAE and contributed significantly towards the performance of depCAE.

Participant-Specific Analysis: As presented in Table III, the type of behaviours of risk varied across participants. Hence, it is crucial to consider the potential dissimilar performance across individuals when training and evaluating behaviours of risk detection methods. Table VI presents the performance of depCAE separately for each participant involved in the study across three cameras. “-” represents the cases where one or less than one agitation window was recorded for the participants. In general, it can be observed that depCAE showed better behaviours of risk detection performance for participants showing less diverse episodes of behaviours of risk, namely, participants 2, 7 and 8, as compared to participants with more diverse episodes. depCAE performed generally well for participant 3 across cameras 1 and 2 and across all three cameras for participant 4, for whom the most number of behaviours of risk windows were recorded. On average, the detection performance was better for participants on cameras 1 and 2 as compared to camera 3.

Sex-Specific Analysis: It is important to investigate the performance of depCAE across population groups. Table VII presents the performance of depCAE stratified based on sex across three cameras. A similar behaviour of risk detection performance was observed for both males and females for Cam1. However, for cameras 2 and 3 it was observed that the depCAE method performed better for females than males. The reason for this can be attributed to the presence of more females than males in the study, leading to the skewed class distribution due to the presence of more behaviours of risk windows for females than males, enhancing the model’s

TABLE VI: depCAE performance stratified over participants.

	Cam1		Cam2		Cam3	
	F1-score	AUROC	F1-score	AUROC	F1-score	AUROC
Participant1	0.239	0.695	0.226	0.669	0.277	0.804
Participant2	0.3	0.895	0.75	0.964	-	-
Participant3	0.345	0.905	0.265	0.742	0.178	0.635
Participant4	0.324	0.878	0.307	0.832	0.274	0.806
Participant5	-	-	-	-	-	-
Participant6	0.276	0.784	-	-	-	-
Participant7	0.32	0.819	-	-	-	-
Participant8	-	-	0.375	0.856	-	-
Participant9	-	-	-	-	-	-
Average	0.3	0.829	0.385	0.813	0.243	0.748

TABLE VII: depCAE performance stratified over sex.

	Cam1		Cam2		Cam3	
	F1-score	AUROC	F1-score	AUROC	F1-score	AUROC
Male (N=2)	0.310	0.837	0.266	0.738	0.160	0.637
Female (N=4)	0.313	0.856	0.294	0.817	0.276	0.806

learning and generalization capabilities for females.

While the study presented important findings for the detection of behaviours of risk in PwD over multiple participants and cameras, there are some limitations associated with the study. First, as the SDU, where the data collection was conducted, usually admits PwD with severe cases of behavioural and psychological symptoms, the number of behaviours of risk episodes displayed by PwD can be higher than a standard LTC facility. Hence, it is crucial to revalidate these findings on the data collected in LTC facilities where the frequency of behaviours of risk episodes is expected to be lower. Second, due to privacy reasons, no camera was installed in private rooms, limiting the analysis of behaviours of risk episodes in public hallways. Hence, the applicability of our findings to more private settings remains unclear. Despite these limitations, our approach effectively detects behaviours of risk episodes with the best AUROC of 0.852, establishing it as the preferred option over existing methods.

V. CONCLUSION AND FUTURE WORK

Caring for individuals with dementia in care settings is increasingly challenging due to growing patient numbers and understaffing issues. The behavioural and psychological symptoms of dementia can lead to incidents that jeopardize the health and safety of patients, staff, and caregivers. Leveraging existing video infrastructure can enable the development of innovative deep-learning approaches to detect such behaviours, thereby preventing injuries and enhancing patient care. As a step in this direction, in this paper, we proposed the depCAE method that uses a novel depth-weighted loss to enforce equivalent importance to both near and far pixels. The depCAE achieved AUROC of 0.852, 0.81 and 0.768 for the three cameras, outperforming any existing methods and recorded lower FPR than baseline 3DCAE method for all three cameras, thus reducing the false alarms for detecting behaviours of risk in PwD. Further, we used the annotation of the training set outliers to determine the operating threshold. Both aspects were critical to depCAE performance and were validated through ablation analysis. This motivates further multidisciplinary research for the deployment of video surveillance-

based behaviours of risk detection systems in nursing and care settings for PwD. Similar multidisciplinary approaches have shown to be helpful in medical settings [25], [26]. A video-based behaviours of risk detection system will help to improve the quality of life for the residents in care homes.

Future work can involve validating our approach on data collected from an LTC that typically encounters fewer behaviours of risk incidents. Pose tracking cameras that directly extract body joints information without recording actual scene [27] can be employed in private areas to detect behaviours of risk in a privacy-protecting manner [4], [28]. It can be a time-consuming and expensive task to train a method separately on each new scene or environment. A lot of time and resources can be saved if a method trained on one scene can generalize well in detecting behaviours of risk in an entirely new scene. Few-shot learning and transfer learning can be employed to improve the performance of depCAE for cross-camera generalization.

In conclusion, this work marks an important step for the development of an automated behaviours of risk detection system that can be employed in real-world care settings and helps to improve the care and safety of PwD in assisted living facilities.

REFERENCES

- [1] J. Cohen-Mansfield, "Instruction manual for the cohen-mansfield agitation inventory (cmai)," *Research Institute of the Hebrew Home of Greater Washington*, vol. 1991, 1991.
- [2] M. of Long-Term Care, "Long-term care staffing study," July 202, <https://www.ontario.ca/page/long-term-care-staffing-study> [Online; accessed 1-March-2023].
- [3] P. K. Mishra, C. Gautam, and A. Tiwari, "Minimum variance embedded auto-associative kernel extreme learning machine for one-class classification," *Neural Computing and Applications*, vol. 33, no. 19, pp. 12973–12987, 2021.
- [4] P. K. Mishra, A. Iaboni, B. Ye, K. Newman, A. Mihailidis, and S. S. Khan, "Privacy-protecting behaviours of risk detection in people with dementia using videos," *BioMedical Engineering OnLine*, vol. 22, no. 1, pp. 1–17, 2023.
- [5] K. Liu and H. Ma, "Exploring background-bias for anomaly detection in surveillance videos," in *Proceedings of the 27th ACM International Conference on Multimedia*, 2019, pp. 1490–1499.
- [6] S. Spasojevic, J. Nogas, A. Iaboni, B. Ye, A. Mihailidis, A. Wang, S. J. Li, L. S. Martin, K. Newman, and S. S. Khan, "A pilot study to detect agitation in people living with dementia using multi-modal sensors," *Journal of Healthcare Informatics Research*, vol. 5, no. 3, pp. 342–358, 2021.
- [7] V. F. S. Fook, P. V. Thang, T. M. Htwe, Q. Qiang, A. A. P. Wai, M. Jayachandran, J. Biswas, and P. Yap, "Automated recognition of complex agitation behavior of dementia patients using video camera," in *2007 9th International Conference on e-Health Networking, Application and Services*. IEEE, 2007, pp. 68–73.
- [8] N. Sharma, J. Klein Brinke, L. Braakman Jansen, P. J. Havinga, and D. V. Le, "Wi-gitation: Replica wi-fi csi dataset for physical agitation activity recognition," *Data*, vol. 9, no. 1, p. 9, 2023.
- [9] Q. Qiu, S. F. Foo, A. A. P. Wai, V. T. Pham, J. Maniyeri, J. Biswas, and P. Yap, "Multimodal information fusion for automated recognition of complex agitation behaviors of dementia patients," in *2007 10th International Conference on Information Fusion*. IEEE, 2007, pp. 1–8.
- [10] B. Chikhaoui, B. Ye, and A. Mihailidis, "Ensemble learning-based algorithms for aggressive and agitated behavior recognition," in *Ubiquitous Computing and Ambient Intelligence*. Cham: Springer International Publishing, 2016, pp. 9–20.
- [11] S. S. Khan, P. K. Mishra, N. Javed, B. Ye, K. Newman, A. Mihailidis, and A. Iaboni, "Unsupervised deep learning to detect agitation from videos in people with dementia," *IEEE Access*, vol. 10, pp. 10349–10358, 2022.

- [12] K. Doshi and Y. Yilmaz, "Online anomaly detection in surveillance videos with asymptotic bound on false alarm rate," *Pattern Recognition*, vol. 114, p. 107865, 2021.
- [13] W. Zhou, Y. Yu, Y. Zhan, and C. Wang, "A vision-based abnormal trajectory detection framework for online traffic incident alert on freeways," *Neural Computing and Applications*, vol. 34, no. 17, pp. 14 945–14 958, 2022.
- [14] M. Mozaffari, K. Doshi, and Y. Yilmaz, "Self-supervised learning for online anomaly detection in high-dimensional data streams," *Electronics*, vol. 12, no. 9, p. 1971, 2023.
- [15] R. Singh, A. Sethi, K. Saini, S. Saurav, A. Tiwari, and S. Singh, "Cvadvan: Constrained video anomaly detection via generative adversarial network," *Image and Vision Computing*, vol. 143, p. 104950, 2024.
- [16] M. Kipp, *Multimedia Annotation, Querying, and Analysis in Anvil*. John Wiley and Sons, Ltd, 2012, ch. 21, pp. 351–367.
- [17] M. L. McHugh, "Interrater reliability: the kappa statistic," *Biochemia Medica*, vol. 22, no. 3, pp. 276–282, 2012.
- [18] K. Krippendorff, "Estimating the reliability, systematic error and random error of interval data," *Educational and Psychological Measurement*, vol. 30, no. 1, pp. 61–70, 1970.
- [19] R. Ranftl, A. Bochkovskiy, and V. Koltun, "Vision transformers for dense prediction," in *Proceedings of the IEEE/CVF international conference on computer vision*, 2021, pp. 12 179–12 188.
- [20] S. S. Khan, P. K. Mishra, B. Ye, K. Newman, A. Iaboni, and A. Mihailidis, "Empirical thresholding on spatio-temporal autoencoders trained on surveillance videos in a dementia care unit," in *2023 20th Conference on robots and vision (CRV)*. IEEE, 2023, pp. 265–272.
- [21] B. Gao, X. Kong, S. Li, Y. Chen, X. Zhang, Z. Liu, and W. Lv, "Enhancing anomaly detection accuracy and interpretability in low-quality and class imbalanced data: A comprehensive approach," *Applied Energy*, vol. 353, p. 122157, 2024.
- [22] N. Madan, N.-C. Ristea, R. T. Ionescu, K. Nasrollahi, F. S. Khan, T. B. Moeslund, and M. Shah, "Self-supervised masked convolutional transformer block for anomaly detection," *IEEE Transactions on Pattern Analysis and Machine Intelligence*, 2023.
- [23] J. Sun, X. Wang, N. Xiong, and J. Shao, "Learning sparse representation with variational auto-encoder for anomaly detection," *IEEE Access*, vol. 6, pp. 33 353–33 361, 2018.
- [24] L. Pinheiro Cinelli, M. Araújo Marins, E. A. Barros da Silva, and S. Lima Netto, *Variational Autoencoder*. Cham: Springer International Publishing, 2021, pp. 111–149. [Online]. Available: https://doi.org/10.1007/978-3-030-70679-1_5
- [25] A. Manji, R. Basiri, F. Harton, K. Rommens, and K. Manji, "Effectiveness of a multidisciplinary limb preservation program in reducing regional hospitalization rates for patients with diabetes-related foot complications," *The International Journal of Lower Extremity Wounds*, p. 15347346241238458, 2024.
- [26] R. Basiri, B. D. Haverstock, P. F. Petrasek, and K. Manji, "Reduction in diabetes-related major amputation rates after implementation of a multidisciplinary model: an evaluation in alberta, canada," *Journal of the American Podiatric Medical Association*, vol. 111, no. 4, 2021.
- [27] AltumView, "Sentinare 2," <https://altumview.ca/>, 2022, [Online; accessed 24-February-2022].
- [28] P. K. Mishra, A. Mihailidis, and S. S. Khan, "Skeletal video anomaly detection using deep learning: Survey, challenges, and future directions," *IEEE Transactions on Emerging Topics in Computational Intelligence*, vol. 8, no. 2, pp. 1073–1085, 2024.



Irene Ballester is a PhD student and research assistant at the Computer Vision Lab at TU Wien, Austria. She is a Marie Curie ITN fellow for the visuAAL project, focusing on developing computer vision models for measuring dementia behaviours. She obtained her Master in Industrial Technology Engineering (specialization in automation and robotics), from the University of Zaragoza, Spain in 2020.



Andrea Iaboni is a geriatric psychiatrist and clinician-scientist. She has a DPhil from Oxford University, UK (2002), and an MD from the University of Toronto, Canada (2006). She completed her residency in psychiatry (FRCPC, 2011) and a fellowship and sub-specialty in geriatric psychiatry (2013). She is an Associate Professor at the University of Toronto and a Senior Scientist at KITE-Toronto Rehab Institute, University Health Network, Toronto, Canada.



Bing Ye, received the MSc. at the Queen's University, Canada. She has over 10 years research experience in aging and technology. Ye has been working as a Research Manager since 2016 in the Intelligent Assistive Technology and Systems Lab (IATSL) at the University of Toronto.



Kristine Newman obtained her Bachelor of Nursing Science (2003) and Master of Science in Nursing (2005) from Queen's University. Dr. Newman completed her PhD in Nursing Science (2012) from the University of Toronto. She is an Associate Professor at the Daphne Cockwell School of Nursing at Toronto Metropolitan University.



Alex Mihailidis, PhD, PEng, is the Barbara G. Stymiest Research Chair in Rehabilitation Technology at KITE Research Institute at University Health Network. He is the Scientific Director of AGE-WELL Network of Centres of Excellence, which focuses on development of new technologies and services for older adults. He is a Professor in the Department of Occupational Science and Occupational Therapy and in the Institute of Biomedical Engineering at the University of Toronto.



Shehroz S. Khan obtained his B.Sc Engineering, Masters and Phd degrees in computer science in 1997, 2010 and 2016. He is currently working as a Scientist at KITE – Toronto Rehabilitation Institute, University Health Network, Canada. He is also cross appointed as an Assistant Professor at the Institute of Biomedical Engineering, University of Toronto.



Pratik K. Mishra obtained his Masters in Computer Science and Engineering from the Indian Institute of Technology Indore, India, in 2020. He is currently pursuing his Ph.D. at the Institute of Biomedical Engineering, University of Toronto. His research is focused towards the application of deep learning for detecting behaviours of risk in patients living with dementia.